Target Localization With Bistatic MIMO and FDA-MIMO Dual-Mode Radar

YUNFEI FANG
Zhoukou Normal University, Zhoukou, China

SHENGQI ZHU, Senior Member, IEEE
Xidian University, Xi'an, China

BIN LIAO, Senior Member, IEEE
Shenzhen University, Shenzhen, China

XIMIN LI
GUISHENG LIAO, Senior Member, IEEE
Xidian University, Xi'an, China

In this article, we investigate the problem of target localization with a multiple-input–multiple-output (MIMO) and frequency diverse array MIMO (FDA-MIMO) dual-mode radar system. The signal model for this newly introduced radar system is presented in detail. On this basis, a computationally efficient method for joint angle and range estimation is proposed by taking advantage of the subspace principle. First, the direction-of-arrival (DOA) of each target is determined by utilizing the fused signal data received via this dual-mode radar. In order to solve the coupling of target range and direction-of-departure (DOD) in FDA-MIMO radar mode, we use the monostatic-like characteristics of the dual-mode radar to develop an effective decoupling method. More specifically, by employing the same eigenmatrix corresponding to MIMO and FDA-MIMO radar data, the coupling of DOD and range in the FDA-MIMO mode can be easily overcome, and the parameters can be successively estimated with automatic paring. Further, to make full use of the transmit array for DOD estimation, we propose to compensate the range information in the transmit array steering vector to achieve an improved estimate of the target DOD. Extensive simulation results are performed to show that the proposed approach can provide superior DOD and range estimation accuracy while maintaining DOA estimation performance under the presented dual-mode radar system, and does not require the design of additional parameter pairing strategies with low computational cost, exhibiting excellent target localization behavior.

Manuscript received 10 February 2023; revised 21 June 2023 and 18 October 2023; accepted 2 November 2023. Date of publication 17 November 2023; date of current version 9 February 2024.

DOI. No. 10.1109/TAES.2023.3333829

Refereeing of this contribution was handled by Justin Metcalf.

This work was supported in part by the National Nature Science Foundation of China undr Grant 62171292, Grant 62211530432, Grant 62101402, Grant 61931016, Grant 62071344, Grant 62201408, Grant 62301404, and Grant 62371377; in part by the Science and Technology Innovation Team of Shaanxi Province under Grant 2022TD-38; in part by the stabilization support of National Radar Signal Processing Laboratory under Grant JKW202108; and in part by the Basic Research Program of Shanxi Province under Grant 202203021212204.

Authors' addresses: Yunfei Fang is with the College of Physics and Telecommunication Engineering, Zhoukou Normal University, Zhoukou 466001, China (e-mail: yunfeifang1991@163.com); Shengqi Zhu, Ximin Li, and Guisheng Liao are with the National Key Laboratory of Radar Signal Processing, Xidian University, Xi'an 710071, China (e-mail: zhushengqi8@163.com; bigboy11272000@126.com; liaogs@xidian.edu.cn); Bin Liao is with the Guangdong Key Laboratory of Intelligent Information Processing, College of Electronics and Information Engineering, Shenzhen University, Shenzhen 518060, China (e-mail: binliao@szu.edu.cn). *(Corresponding author: Shengqi Zhu.)*

0018-9251

I. INTRODUCTION

Target localization is a crucial research topic in the military and civilian fields [1], [2], [3], [4]. The advantage of the directional gain provided via phased array makes it extremely attractive for improving the performance of radar systems. Unlike phased array radar, the multiple-input–multiple-output (MIMO) radar can employ the spatial diversity offered by emitting orthogonal waveforms and the extended virtual array formed by combining transmit and receive antennas, which makes it occupy the merit of resolution enhancement and fading mitigation [5], [6], [7], [8]. However, both phased array and MIMO radars exhibit only angle-dependent transmit patterns. This results in them not being particularly effective in scenarios with range-dependent targets or undesired interferences [9], [10], [11], [12].

A more capable array radar, referred to as frequency diverse array (FDA), was presented in [13], [14], [15], and [16]. Unlike traditional MIMO radar that can only identify targets from the temporal domain and spatial domain, FDA radar achieves a range-angle-time-dependent beampattern by applying a small frequency offset across the transmit antenna [17], [18], [19]. This enables it to provide a more flexible way to identify the target signal or interference from the multidimensional domain. In view of this, FDA radar has received extensive attention in the fields of target localization [20], [21], [22], high-resolution imaging [23], [24], [25], interference and clutter suppression [26], [27], [28].

It is well known that the coupling of range and angle in the transmit steering vector is an inherent problem in FDA radar. This makes attempts to locate targets by exploiting the range-dimensional advantages of FDA radars relatively unsatisfactory. To this end, a dual-pulse target localization method for FDA radar is developed in [29], where zero and nonzero frequency offsets are employed to achieve the angle and range estimation of the target signal, respectively. Subsequently, a subarray-based target localization method is devised in [30]. This method achieves the corresponding decoupling using two subarrays with different frequency offsets, which is similar to the strategy in [29]. Note that the approach in [30] decouples range and angle from the perspective of subarrays. This virtually reduces the effective array aperture for target parameter estimation. Furthermore, by means of discrete spheroidal sequence a beam pattern synthesis scheme is presented in [31], which decouples the intertwining relationship between range and angle. In [32], by leveraging multiple subarrays a transmit subaperturing technique for FDA radar is derived to achieve range and angle distinction, but herein the loss of array aperture is still unavoidable. Using the maximum likelihood estimator, a target localization approach based on FDA radar for joint estimation of range and angle is proposed in [33]. In this method, the target localization problem is reformulated as a spectrum estimation one, and the range ambiguity is also solved by a designed frequency increment. Note that although this method exhibits excellent target localization performance, it has a considerable computational burden. Moreover, a large number of techniques using nonlinear frequency shift have also been developed to improve the performance of FDA radar from various perspectives, for instance, logarithmically frequency offsets [34], random frequency offsets [35], and coprime frequency offsets [36].

It is a natural fact that these methods mentioned above exhibit outstanding target localization performance with the spatial diversity and higher degrees of freedom provided via MIMO radar. However, they only work with monostatic FDA-MIMO radar. This is mainly based on the fact that in this scenario the coupling of range and angle in the transmit steering vector can be disentangled by the angle estimation obtained from the receive steering vector. In fact, in the bistatic FDA-MIMO radar scenario the decoupling of the range and angle in the transmit steering vector is more complicated due to the difference in the direction-of-departure (DOD) and direction-of-arrival (DOA) of the target signal.

In order to solve the coupling of range and angle in the transmit steering vector under bistatic FDA-MIMO radar, a search-free target localization method is derived [37]. This approach utilizes nonlinear frequency offset to decouple range and angle, and gives the corresponding phase ambiguity resolving approach. In [38], a real-valued subspace decomposition-based target localization method for bistatic FDA-MIMO radar is proposed, which exploits real-valued rotation invariance to reduce the corresponding computational complexity. However, the methods in [37] and [38] are based on the routine of dividing the entire array into multiple subarrays, and require additional pairings to ensure that they can be applied to multitarget scenarios. In [39], a joint space-time-frequency domain target localization method is established. This method can achieve the purpose of synthesizing multiple subarrays by employing multiple coprime frequency increments, providing larger array aperture and signal bandwidth. Note that although this method does not require an additional pairing process, the principle is also to use multiple subarrays to achieve the decoupling of range and DOD. At the same time, the use of coprime frequency increments and arrays increases the design complexity of radar system. Furthermore, in [40] a space-time adaptive processing method based on bistatic FDA-MIMO radar is developed to achieve clutter suppression.

In this article, we construct a dual-mode radar system combining MIMO and FDA-MIMO radar and propose an automatic decoupled target localization method. In our proposed approach, the MIMO and FDA-MIMO dual-mode radar system is first designed, and the corresponding received signals for dual-mode radar are obtained. With this fused signal data, the estimation of signal parameters via rotation invariance techniques (ESPRIT) [41] is utilized to achieve DOA estimation of the target signal. In order to overcome the inconsistency of the phase of the estimated transmit steering vector in MIMO and FDA-MIMO radar modes, the eigenmatrix obtained from the dual-mode radar data is applied to the subspace data corresponding to the two radar modes, respectively. In this way, we can perfectly register the phase corresponding to the transmit steering vector of the same target in different radar modes. Then, by synthesizing the DOD information estimated in the MIMO radar mode into the FDA-MIMO radar mode, we can directly calculate the range parameter of the target signal. This straightforwardly eliminates the coupling of range and angle in the transmit steering vector in FDA-MIMO radar mode, and does not require additional pairing. Moreover, by relying on a designed range compensation factor we also derive an enhanced DOD estimation algorithm that can comprehensively utilize all the transmit steering vector information of this dual-mode radar to achieve considerable performance improvement.

The essence of our method is to use the DOD information of the target signal provided via the MIMO radar to solve the range-angle coupling in the FDA-MIMO radar. This advantage is that in MIMO and FDA-MIMO dual-mode radar, it can not only solve the coupling of range and angle but also significantly enhance the DOD and range estimation performance. Meanwhile, the designed dual-mode radar synergy scheme is considerable attractive in both simplifying the radar system design and reducing the computational complexity. The simulation results show that the proposed method can provide more outstanding range and DOD estimation performance while ensuring the DOA estimation performance of the target signal compared with the existing target localization methods under the bistatic FDA-MIMO radar, and has lower computational complexity.

The rest of this article is organized as follows. Section II presents the signal model of the designed MIMO and FDA-MIMO dual-mode radar. The target parameter estimation method for bistatic MIMO and FDA-MIMO radar are shown in Section III, including range, DOD, and DOA estimation of target signal as well as the range compensation approach. Simulation results are provided in Section IV to evaluate the performance of the proposed target localization method based on MIMO and FDA-MIMO dual-mode radar. Finally, Section V concludes of this article.

Notations: $(\cdot)^*$, $(\cdot)^T$, $(\cdot)^H$, and $(\cdot)^{-1}$ represent the conjugate, transpose, conjugate–transpose, inverse transformation, respectively. $\otimes$, $\odot$, and $\circ$ stand for the Kronecker product, Khatri–Rao product, and elementwise operation,

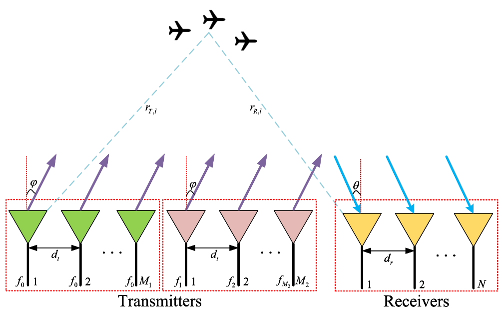

Fig. 1. Illustration of MIMO and FDA-MIMO dual-mode radar system.

respectively. $E\{\cdot\}$ denotes the expectation operation. $\mathrm{diag}\{\cdot\}$ means a diagonalization operation. $\arg(\cdot)$ stands for the operation of taking the phase angle. $\mathbf{I}_M$ denotes the $M \times M$ identity matrix and $\mathbf{0}_{M\times N}$ is the zero matrix of size $M \times N$.

II. SIGNAL MODEL OF DUAL-MODE RADAR

As shown in Fig. 1, we consider a dual-mode radar system consisting of MIMO radar and FDA-MIMO radar. Here, the triangles with green and pink denote the transmit antennas of the MIMO radar and the FDA-MIMO radar, respectively, and the triangles with yellow represent the receive antennas of this dual-mode radar. φ and θ are the DOD and DOA information of the target, respectively. Specifically, the transmitters of MIMO radar and FDA-MIMO radar are equipped with M_1 and M_2 antennas, respectively. The total number of transmit antennas of the dual-mode radar system is $M = M_1 + M_2$. The receiver is deployed with N antennas. Let the first antenna of the MIMO radar be the reference, the transmitted signal corresponding to MIMO radar and FDA-MIMO radar in this dual-mode system can thus be expressed, respectively, as

$$s_{1,m'}(t) = \mathrm{rect}\left(\tfrac{t}{T_p}\right)\phi_{1,m'}(t)e^{j2\pi f_0 t},\ \ m' = 1, 2, \ldots, M_1 \tag{1a}$$

$$s_{2,m}(t) = \mathrm{rect}\left(\tfrac{t}{T_p}\right)\phi_{2,m}(t)e^{j2\pi f_m t},\ \ m = 1, 2, \ldots, M_2 \tag{1b}$$

where $\mathrm{rect}\left(\tfrac{t}{T_p}\right)$ with $0 \le t \le T_p$ denotes the pulse function and T_p is the pulse width, $\phi_{1,m'}(t)$ and $\phi_{2,m}(t)$ are the waveforms associated with the m'th antenna of MIMO radar and mth antenna of FDA-MIMO radar, respectively, and they are assumed to be orthogonal. f_0 is the MIMO radar carrier frequency and f_m is the carrier frequency on the mth element of the FDA-MIMO radar. Moreover, we have

$$f_m = f_0 + (m-1)\Delta f \tag{2}$$

where Δf is the frequency offset of FDA-MIMO radar and is much smaller than f_0, i.e., $\Delta f \ll f_0$.

In this article, both the antennas in the transmitter and receiver are uniformly and linearly arranged with interelement spacings being d_t and d_r, respectively. Furthermore, we assume $d_t = d_r = d = \lambda_{\min}/2$, where $\lambda_{\min}$ denotes the minimum wavelength, such that the phase ambiguity issue can be avoided. Suppose that there are L uncorrelated targets from the far field with spatial locations $\{r_l, \varphi_l, \theta_l\}_{l=1}^{L}$, where r_l, φ_l, and θ_l are the range, DOD, and DOA, respectively. Note also that the L targets are assumed to be in the same range cell. The received signal by the nth antenna from the lth target can be expressed as

$$y_{n,l} = y_{1,n,l} + y_{2,n,l} \tag{3}$$

where $y_{1,n,l}$ and $y_{2,n,l}$ are the components associated with the MIMO and FDA-MIMO, respectively, and they are given by

$$\begin{aligned} y_{1,n,l} = &\sum_{m'=1}^{M_1} \xi_l \mathrm{rect}\left(\tfrac{t-\tau_0}{T_p}\right)\phi_{1,m'}\left(t - \tau_{1,m',l} - \tilde{\tau}_{n,l}\right) \\ &\cdot e^{j2\pi f_0\left(t-\tau_{1,m',l}-\tilde{\tau}_{n,l}\right)} \end{aligned} \tag{4a}$$

$$\begin{aligned} y_{2,n,l} = &\sum_{m=1}^{M_2} \xi_l \mathrm{rect}\left(\tfrac{t-\tau_0}{T_p}\right)\phi_{2,m}\left(t - \tau_{2,m,l} - \tilde{\tau}_{n,l}\right) \\ &\cdot e^{j2\pi f_m\left(t-\tau_{2,m,l}-\tilde{\tau}_{n,l}\right)} \end{aligned} \tag{4b}$$

where ξ_l is the reflection coefficient of the lth target.

In (4), $\tau_{1,m',l}$ ($\tau_{2,m,l}$) and $\tilde{\tau}_{n,l}$ stand for, respectively, the time delay from the m'th (mth) transmit antenna of the MIMO radar (FDA-MIMO radar) to the lth target and the time delay from the lth target to the nth receive antenna, respectively. They can be written out as

$$\tau_{1,m',l} = \tfrac{1}{c}\left[r_{T,l} - d_t\left(m'-1\right)\sin\varphi_l\right] \tag{5a}$$

$$\tau_{2,m,l} = \tfrac{1}{c}\left[r_{T,l} - d_t\left(m+M_1-1\right)\sin\varphi_l\right] \tag{5b}$$

$$\tilde{\tau}_{n,l} = \tfrac{1}{c}\left[r_{R,l} - d_r(n-1)\sin\theta_l\right] \tag{5c}$$

where $r_{T,l}$ and $r_{R,l}$ denote the ranges from the lth target to the reference transmit antenna and receive antenna, respectively.

At the receiver side, after downconversion and matched filtering, $y_{1,n,l}$ and $y_{2,n,l}$ becomes

$$y_{1,nm',l} \approx \xi_l e^{j2\pi\frac{f_0}{c}\left[d\left(m'-1\right)\sin(\varphi_l) + d(n-1)\sin(\theta_l)\right]} \tag{6a}$$

$$\begin{aligned} y_{2,nm,l} \approx\ &\xi_l e^{-j2\pi\frac{f_0}{c}r_l} e^{j2\pi\frac{M_1 d f_0 \sin(\theta_l)}{c}} \\ &\cdot e^{-j2\pi\frac{\Delta f}{c}(m-1)r_l} e^{j2\pi\frac{f_0}{c}\left[d(m-1)\sin(\varphi_l)+d(n-1)\sin(\theta_l)\right]} \end{aligned} \tag{6b}$$

where $r_l = r_{T,l} + r_{R,l}$ denotes the range of the lth target. Note that the establishment of (6b) relies on the premise that $\Delta f \ll f_0$ [17]. Therefore, the outputs $\mathbf{y}_{1,n,l} \in \mathbb{C}^{M_1\times 1}$ and $\mathbf{y}_{2,n,l} \in \mathbb{C}^{M_2\times 1}$ (associated with the lth target) of the nth receive element corresponding to MIMO radar and FDA-MIMO radar can be expressed, respectively, as

$$\mathbf{y}_{1,n,l} = \xi_l e^{j2\pi\frac{d}{\lambda_0}(n-1)\sin(\theta_l)} \begin{bmatrix} 1 \\ e^{j2\pi\frac{d}{\lambda_0}\sin(\varphi_l)} \\ \vdots \\ e^{j2\pi\frac{d}{\lambda_0}(M_1-1)\sin(\varphi_l)} \end{bmatrix} \tag{7a}$$

$$\mathbf{y}_{2,n,l} = \xi_l \eta_l e^{j2\pi\frac{d}{\lambda_0}(n-1)\sin(\theta_l)}$$

$$\cdot\begin{bmatrix} 1 \\ e^{-j2\pi\frac{\Delta f}{c}r_l+j2\pi\frac{d}{\lambda_0}\sin(\varphi_l)} \\ \vdots \\ e^{-j2\pi\frac{\Delta f}{c}(M_2-1)r_l+j2\pi\frac{d}{\lambda_0}(M_2-1)\sin(\varphi_l)} \end{bmatrix} \tag{7b}$$

where $\eta_l = e^{-j2\pi\frac{f_0}{c}r_l}\cdot e^{j2\pi\frac{M_1 d f_0 \sin(\varphi_l)}{c}}$.

By stacking the outputs of the N array elements, the final output signals of the MIMO radar and FDA-MIMO radar can be rewritten, respectively, as

$$\mathbf{x}_1(t) = \mathbf{A}_1\mathbf{s}(t) \tag{8a}$$

$$\mathbf{x}_2(t) = \mathbf{A}_2\mathbf{s}(t) \tag{8b}$$

where $\mathbf{A}_1 = [\mathbf{a}_1(\varphi_1,\theta_1), \mathbf{a}_1(\varphi_2,\theta_2), \ldots, \mathbf{a}_1(\varphi_L,\theta_L)] \in \mathbb{C}^{M_1N\times L}$ and $\mathbf{A}_2 = [\mathbf{a}_2(r_1,\varphi_1,\theta_1), \mathbf{a}_2(r_2,\varphi_2,\theta_2), \ldots, \mathbf{a}_2(r_L,\varphi_L,\theta_L)] \in \mathbb{C}^{M_2N\times L}$ are the array steering matrices corresponding to MIMO radar and FDA-MIMO radar, respectively. $\mathbf{s}(t) = [\xi_1(t), \xi_2(t), \ldots, \xi_L(t)]^T \in \mathbb{C}^{L\times 1}$ stands for the equivalent reflection coefficient of the L targets. $\mathbf{a}_1(\varphi_l,\theta_l) \in \mathbb{C}^{M_1N\times 1}$ and $\mathbf{a}_2(r_l,\varphi_l,\theta_l) \in \mathbb{C}^{M_2N\times 1}$ are the corresponding steering vectors, both of which can be given as

$$\mathbf{a}_1(\varphi_l,\theta_l) = \mathbf{a}_{\mathrm{t}1}(\varphi_l)\otimes\mathbf{a}_{\mathrm{r}}(\theta_l) \tag{9a}$$

$$\mathbf{a}_2(r_l,\varphi_l,\theta_l) = \mathbf{a}_{\mathrm{t}2}(r_l,\varphi_l)\otimes\mathbf{a}_{\mathrm{r}}(\theta_l) \tag{9b}$$

where $\mathbf{a}_{\mathrm{r}}(\theta) \in \mathbb{C}^{N\times 1}$ is the receive steering vector defined as

$$\mathbf{a}_{\mathrm{r}}(\theta_l) = \left[1, e^{j2\pi\frac{d}{\lambda_0}\sin(\theta_l)}, \ldots, e^{j2\pi\frac{d}{\lambda_0}(N-1)\sin(\theta_l)}\right]^T \tag{10}$$

and $\mathbf{a}_{\mathrm{t}1}(\varphi_l) \in \mathbb{C}^{M_1\times 1}$ and $\mathbf{a}_{\mathrm{t}2}(r_l,\varphi_l) \in \mathbb{C}^{M_2\times 1}$ denote the transmit steering vectors corresponding to MIMO radar and FDA-MIMO radar, respectively, as

$$\mathbf{a}_{\mathrm{t}1}(\varphi_l) = \left[1, e^{j2\pi\frac{d}{\lambda_0}\sin(\varphi_l)}, \ldots, e^{j2\pi\frac{d}{\lambda_0}(M_1-1)\sin(\varphi_l)}\right]^T \tag{11a}$$

$$\mathbf{a}_{\mathrm{t}2}(r_l,\varphi_l) = \eta_l\begin{bmatrix} 1 \\ e^{-j2\pi\frac{\Delta f}{c}r_l+j2\pi\frac{d}{\lambda_0}\sin(\varphi_l)} \\ \vdots \\ e^{-j2\pi\frac{\Delta f}{c}(M_2-1)r_l+j2\pi\frac{d}{\lambda_0}(M_2-1)\sin(\varphi_l)} \end{bmatrix}. \tag{11b}$$

Now, taking the noise into account, the ultimately received signal $\mathbf{x}(t)$ of MIMO and FDA-MIMO dual-mode radar can be modeled as

$$\mathbf{x}(t) = \begin{bmatrix}\mathbf{x}_1(t)\\ \mathbf{x}_2(t)\end{bmatrix} + \mathbf{n}(t) = \mathbf{A}\mathbf{s}(t) + \mathbf{n}(t) \tag{12}$$

where $\mathbf{n}(t)$ denotes the complex white Gaussian noise with zero-mean and variance σ^2, which is assumed to be uncorrelated with the target signal. In addition, $\mathbf{A} \in \mathbb{C}^{MN\times L}$ is the joint steering matrix of the MIMO and FDA-MIMO radars, and it can be expressed as

$$\begin{aligned}\mathbf{A} &\triangleq \begin{bmatrix}\mathbf{A}_1\\ \mathbf{A}_2\end{bmatrix} \\ &= [\mathbf{a}_{\mathrm{t}}(r_1,\varphi_1)\otimes\mathbf{a}_{\mathrm{r}}(\theta_1), \ldots, \mathbf{a}_{\mathrm{t}}(r_L,\varphi_L)\otimes\mathbf{a}_{\mathrm{r}}(\theta_L)] \\ &= [\mathbf{a}_{\mathrm{t}}(r_1,\varphi_1), \ldots, \mathbf{a}_{\mathrm{t}}(r_L,\varphi_L)]\otimes\mathbf{a}_{\mathrm{r}}(\theta_L)\end{aligned} \tag{13}$$

with

$$\mathbf{a}_{\mathrm{t}}(r_l,\varphi_l) = [\mathbf{a}_{\mathrm{t}1}^T(\varphi_l), \mathbf{a}_{\mathrm{t}2}^T(r_l,\varphi_l)]^T. \tag{14}$$

According to the above model, we can obtain the covariance matrix of the received echo with the dual-mode radar as

$$\mathbf{R}_x = E\left\{\mathbf{x}(t)\mathbf{x}^H(t)\right\} = \mathbf{R}_s + \mathbf{Q} \tag{15}$$

where $\mathbf{R}_s = \mathbf{A}E\{\mathbf{s}(t)\mathbf{s}^H(t)\}\mathbf{A}^H \in \mathbb{C}^{MN\times MN}$, and $\mathbf{Q} = \sigma^2\mathbf{I}_{MN}$ is the noise covariance matrix. In practice, considering the finite number of sampling snapshots, the covariance matrix $\mathbf{R}_x$ can be estimated as: $\hat{\mathbf{R}}_x = \frac{1}{J}\sum_{t_j=1}^{J}\mathbf{x}(t_j)\mathbf{x}^H(t_j)$, where J is the number of snapshots. The eigen-decomposition of $\mathbf{R}_x$ can be expressed as follows:

$$\mathbf{R}_x = \mathbf{U}_s\mathbf{\Lambda}_s\mathbf{U}_s^H + \mathbf{U}_n\mathbf{\Lambda}_n\mathbf{U}_n^H \tag{16}$$

where $\mathbf{U}_s \in \mathbb{C}^{MN\times L}$ denotes the signal subspace composed of the eigenvectors associated with the L largest eigenvalues which forms the diagonal matrix $\mathbf{\Lambda}_s \in \mathbb{C}^{L\times L}$, and $\mathbf{U}_n \in \mathbb{C}^{MN\times(MN-L)}$ denotes the noise subspace composed of the eigenvectors associated with the $MN-L$ smallest eigenvalues which forms the diagonal matrix $\mathbf{\Lambda}_n \in \mathbb{C}^{(MN-L)\times(MN-L)}$. Note that the number of targets is assumed to be known a priori or can be efficiently estimated by some existing techniques.

III. TARGET PARAMETER ESTIMATION FOR BISTATIC MIMO AND FDA-MIMO DUAL-MODE RADAR

In this section, we present the proposed method for DOA, DOD, and range estimation by taking advantage of the dual-mode architecture of the radar system.

A. DOA Estimation

According to the subspace theory, the signal subspace $\mathbf{U}_s$ spans the same space as $\mathbf{A}$. Thus, there exists a nonsingular matrix $\mathbf{T} \in \mathbb{C}^{L\times L}$ such that $\mathbf{U}_s = \mathbf{AT}$. Then, let us define two matrices $\mathbf{U}_{sr1} \in \mathbb{C}^{M(N-1)\times L}$ and $\mathbf{U}_{sr2} \in \mathbb{C}^{M(N-1)\times L}$, which are extracted from $\mathbf{U}_s$ as

$$\mathbf{U}_{sr1} = \mathbf{J}_1\mathbf{U}_s = \mathbf{J}_1\mathbf{AT} \tag{17a}$$

$$\mathbf{U}_{sr2} = \mathbf{J}_2\mathbf{U}_s = \mathbf{J}_2\mathbf{AT} \tag{17b}$$

where $\mathbf{J}_1 = \mathbf{I}_M\otimes[\mathbf{I}_{(N-1)}, \mathbf{0}_{(N-1)\times 1}]$ and $\mathbf{J}_2 = \mathbf{I}_M\otimes[\mathbf{0}_{(N-1)\times 1}, \mathbf{I}_{(N-1)}]$. Recalling the definition of $\mathbf{A}$ in (13), it can be readily obtained that

$$\mathbf{J}_2\mathbf{A} = \mathbf{J}_1\mathbf{A}\mathbf{\Phi}_r \tag{18}$$

where $\mathbf{\Phi}_r \in \mathbb{C}^{L\times L}$ is a diagonal matrix and it is given by

$$\mathbf{\Phi}_r = \mathrm{diag}\left\{e^{j2\pi\frac{d}{\lambda_0}\sin(\theta_1)}, \ldots, e^{j2\pi\frac{d}{\lambda_0}\sin(\theta_L)}\right\}. \tag{19}$$

Inserting (18) into (17) yields

$$\mathbf{T}^{-1}\mathbf{\Phi}_r\mathbf{T} = \left(\mathbf{U}_{sr1}^H\mathbf{U}_{sr1}\right)^{-1}\mathbf{U}_{sr1}^H\mathbf{U}_{sr2} \triangleq \mathbf{\Psi}_r \tag{20}$$

which indicates that $\mathbf{\Phi}_r$ and $\mathbf{\Psi}_r$ are similar matrices. This shows that the diagonal elements of matrix $\mathbf{\Phi}_r$ are eigenvalues of $\mathbf{\Psi}_r$. As a consequence, performing an eigen-decomposition on the matrix $\mathbf{\Psi}_r$, we have

$$\mathbf{\Psi}_r = \mathbf{G}_r\tilde{\mathbf{\Phi}}_r\mathbf{G}_r^{-1} \tag{21}$$

where $\tilde{\boldsymbol{\Phi}}_r = \text{diag}\{\tilde{v}_{r1}, \tilde{v}_{r2}, \ldots, \tilde{v}_{rL}\} \in \mathbb{C}^{L\times L}$ denotes a diagonal matrix composed of L eigenvalues of $\boldsymbol{\Psi}_r$, and $\mathbf{G}_r$ is the corresponding eigenmatrix. Therefore, the DOA of the target signal can be estimated as

$$\hat{\theta}_l = \arcsin\left(\frac{\lambda_0 \arg(\tilde{v}_{rl})}{2\pi d}\right). \tag{22}$$

It is worth mentioning that both $\mathbf{T}^{-1}$ and $\mathbf{G}_r$ are eigenmatrices of $\boldsymbol{\Psi}_r$, and their corresponding eigenvalue matrices $\boldsymbol{\Phi}_r$ and $\tilde{\boldsymbol{\Phi}}_r$ are identical except the different order of diagonal entries.

B. DOD and Range Estimation

Traditionally, the problem of DOD and range estimation is not easy due to their coupling. However, in this subsection, this problem can be simply resolved with the dual mode.

1) *DOD Estimation Based on MIMO Radar Mode:* From (13) and using the fact that $\mathbf{U}_s = \mathbf{AT}$, we have

$$\mathbf{U}_s = \begin{bmatrix}\mathbf{A}_1\\ \mathbf{A}_2\end{bmatrix}\mathbf{T} = \begin{bmatrix}\mathbf{U}_{1,s}\\ \mathbf{U}_{2,s}\end{bmatrix} \tag{23}$$

where $\mathbf{U}_{1,s} = \mathbf{A}_1\mathbf{T}$, $\mathbf{U}_{2,s} = \mathbf{A}_2\mathbf{T}$. It is noticed that $\mathbf{U}_{1,s}$ and $\mathbf{U}_{2,s}$ corresponds to the first $M_1 N$ and the last $M_2 N$ rows of $\mathbf{U}_s$, respectively. Following the strategy in Section II-I-A, let us define $\mathbf{P}_1 = [\mathbf{I}_{(M_1-1)}, \mathbf{0}_{(M_1-1)\times 1}] \otimes \mathbf{I}_N$ and $\mathbf{P}_2 = [\mathbf{0}_{(M_1-1)\times 1}, \mathbf{I}_{(M_1-1)}] \otimes \mathbf{I}_N$, and we have

$$\mathbf{P}_2\mathbf{A}_1 = \mathbf{P}_1\mathbf{A}_1\boldsymbol{\Phi}_{1,t} \tag{24}$$

where

$$\boldsymbol{\Phi}_{1,t} = \text{diag}\left\{e^{j2\pi\frac{d}{\lambda_0}\sin(\varphi_1)}, \ldots, e^{j2\pi\frac{d}{\lambda_0}\sin(\varphi_L)}\right\}. \tag{25}$$

Accordingly, we obtain two matrices $\mathbf{U}_{1,st1} \in \mathbb{C}^{(M_1-1)N\times L}$ and $\mathbf{U}_{1,st2} \in \mathbb{C}^{(M_1-1)N\times L}$ as

$$\mathbf{U}_{1,st1} = \mathbf{P}_1\mathbf{U}_{1,s} = \mathbf{P}_1\mathbf{A}_1\mathbf{T} \tag{26a}$$

$$\mathbf{U}_{1,st2} = \mathbf{P}_2\mathbf{U}_{1,s} = \mathbf{P}_2\mathbf{A}_2\mathbf{T} = \mathbf{P}_1\mathbf{A}_1\boldsymbol{\Phi}_{1,t}\mathbf{T} \tag{26b}$$

which implies that

$$\mathbf{T}^{-1}\boldsymbol{\Phi}_{1,t}\mathbf{T} = \left(\mathbf{U}_{1,st1}^H\mathbf{U}_{1,st1}\right)^{-1}\mathbf{U}_{1,st1}^H\mathbf{U}_{1,st2} \triangleq \boldsymbol{\Psi}_{1,t}. \tag{27}$$

From (20) and (27), it is known that $\boldsymbol{\Psi}_{1,t}$ and $\boldsymbol{\Psi}_r$ share the same eigenmatrix. For a given eigenmatrix $\mathbf{T}^{-1}$, we have $\boldsymbol{\Phi}_{1,t} = \mathbf{T}\boldsymbol{\Psi}_{1,t}\mathbf{T}^{-1}$, and for a given eigenmatrix $\mathbf{G}_r$, we have

$$\tilde{\boldsymbol{\Phi}}_{1,t} = \mathbf{G}_r^{-1}\boldsymbol{\Psi}_{1,t}\mathbf{G}_r \tag{28}$$

which is identical to $\boldsymbol{\Phi}_{1,t}$ except the different order of diagonal entries. Thus, let $\tilde{\boldsymbol{\Phi}}_{1,t} = \text{diag}\{\tilde{v}_{t1}, \tilde{v}_{t2}, \ldots, \tilde{v}_{tL}\}$, then the DOD can be determined by the MIMO radar mode as

$$\hat{\varphi}_l = \arcsin\left(\frac{\lambda_0 \arg(\tilde{v}_{tl})}{2\pi d}\right). \tag{29}$$

Note that the orders of diagonal entries of $\tilde{\boldsymbol{\Phi}}_r$ and $\tilde{\boldsymbol{\Phi}}_{1,t}$ are determined by the same eigenmatrix, the DOA and DOD obtained by (22) and (29) are automatically paired and corresponding to the same target.

2) *Range Estimation Based on FDA-MIMO Radar Mode:* In a similar way, let us define $\mathbf{Q}_1 = [\mathbf{I}_{(M_2-1)}, \mathbf{0}_{(M_2-1)\times 1}] \otimes \mathbf{I}_N$ and $\mathbf{Q}_2 = [\mathbf{0}_{(M_2-1)\times 1}, \mathbf{I}_{(M_2-1)}] \otimes \mathbf{I}_N$, and obtain two submatrices $\mathbf{U}_{2,st1} \in \mathbb{C}^{(M_2-1)N\times L}$ and $\mathbf{U}_{2,st2} \in \mathbb{C}^{(M_2-1)N\times L}$ from $\mathbf{U}_{2,s}$ as follows:

$$\mathbf{U}_{2,st1} = \mathbf{Q}_1\mathbf{U}_{2,s} = \mathbf{Q}_1\mathbf{A}_2\mathbf{T} \tag{30a}$$

$$\mathbf{U}_{2,st2} = \mathbf{Q}_2\mathbf{U}_{2,s} = \mathbf{Q}_2\mathbf{A}_2\mathbf{T} = \mathbf{Q}_1\mathbf{A}_2\boldsymbol{\Phi}_{2,t}\mathbf{T} \tag{30b}$$

where we have used the fact that $\mathbf{Q}_2\mathbf{A}_2 = \mathbf{Q}_1\mathbf{A}_2\boldsymbol{\Phi}_{2,t}$ with

$$\boldsymbol{\Phi}_{2,t} = \text{diag}\left\{e^{-j2\pi\frac{\Delta f}{c}r_1 + j2\pi\frac{d}{\lambda_0}\sin(\varphi_1)}, \ldots, e^{-j2\pi\frac{\Delta f}{c}r_L + j2\pi\frac{d}{\lambda_0}\sin(\varphi_L)}\right\}. \tag{31}$$

According to (30), we have

$$\mathbf{T}^{-1}\boldsymbol{\Phi}_{2,t}\mathbf{T} = \left(\mathbf{U}_{2,st1}^H\mathbf{U}_{2,st1}\right)^{-1}\mathbf{U}_{2,st1}^H\mathbf{U}_{2,st2} \triangleq \boldsymbol{\Psi}_{2,t} \tag{32}$$

and for the given eigenamtrix $\mathbf{G}_r$ (rather than $\mathbf{T}^{-1}$), a diagonal matrix $\tilde{\boldsymbol{\Phi}}_{2,t}$ with reordered diagonal entries of $\boldsymbol{\Phi}_{2,t}$ can be obtained as

$$\tilde{\boldsymbol{\Phi}}_{2,t} = \mathbf{G}_r^{-1}\boldsymbol{\Psi}_{2,t}\mathbf{G}_r. \tag{33}$$

Recalling the definitions of $\boldsymbol{\Phi}_{1,t}$ and $\boldsymbol{\Phi}_{2,t}$ in (25) and (31), we can obtain a diagonal matrix $\boldsymbol{\Gamma} = \text{diag}\{\gamma_1, \ldots, \gamma_L\}$ as

$$\boldsymbol{\Gamma} = \boldsymbol{\Phi}_{1,t}\boldsymbol{\Phi}_{2,t}^{-1} = \text{diag}\left\{e^{j2\pi\frac{\Delta f}{c}r_1}, \ldots, e^{j2\pi\frac{\Delta f}{c}r_L}\right\} \tag{34}$$

which contains the information of the targets in the phases of the diagonal entries. Generally speaking, FDA-MIMO radars utilize a small frequency offset across transmit elements to achieve a range-dependent transmit beampattern. In order to effectively obtain a range estimation of the target signal, the range r_l should be constrained to $(0, c/\Delta f)$ [33]. Therefore, the term $2\pi\Delta f r_l/c$ in the transmit steering vector with FDA-MIMO radar mode should satisfy $0 < 2\pi\Delta f r_l/c < 2\pi$. Under this condition, we can determine the range of the target as $r_l = \frac{c}{2\pi\Delta f}\arg(\gamma_l)$, where $\arg(\cdot)$ returns the phase within $(0, 2\pi]$.

Similar to the angle estimation, given the eigenmatrix $\mathbf{G}_r$, we can only obtain a diagonal matrix

$$\tilde{\boldsymbol{\Gamma}} = \tilde{\boldsymbol{\Phi}}_{1,t}\tilde{\boldsymbol{\Phi}}_{2,t}^{-1} = \text{diag}\{\tilde{\gamma}_1, \ldots, \tilde{\gamma}_L\} \tag{35}$$

which has the same diagonal entries as $\boldsymbol{\Gamma}$, but their orders of the diagonal sequences are different. Thus, the range of the target is estimated as

$$\hat{r}_l = \frac{c}{2\pi\Delta f}\arg(\tilde{\gamma}_l) \tag{36}$$

which can automatically pair with $\hat{\theta}_l$ and $\hat{\varphi}_l$ for the same target.

3) *Improved DOD Estimation Based on MIMO and FDA-MIMO Dual-Mode:* It can be seen that, the DOD estimation based on MIMO radar mode only uses part of the transmit array. For MIMO radar, if a larger transmit antenna array or more antennas can be used, the DOD can be estimated more accurately. In other words, the performance of angle estimation depends on the array aperture. This motivates us to make full use of the transmit antennas

for MIMO radar and FDA-MIMO radar. From (11b), it is seen that the transmit steering vector of the MIMO and FDA-MIMO dual-mode radar is dependent on both the DOD and range of the target. Moreover, steering vector $\mathbf{a}_{t2}(r_l, \varphi_l)$ of the FDA-MIMO radar can be rewritten as

$$\mathbf{a}_{t2}(r_l, \varphi_l) = \mathbf{r}_l \odot \mathbf{a}'_{t2}(\varphi_l) \tag{37}$$

where

$$\mathbf{r}_l = e^{-j2\pi \frac{f_0}{c} r_l} \left[1, e^{-j2\pi \frac{\Delta f}{c} r_l}, \ldots, e^{-j2\pi \frac{\Delta f}{c}(M_2-1) r_l}\right]^T \tag{38}$$

and

$$\mathbf{a}'_{t2}(\varphi_l) = e^{j2\pi \frac{M_1 d f_0 \sin(\varphi_l)}{c}} \begin{bmatrix} 1 \\ e^{j2\pi \frac{d}{\lambda_0} \sin(\varphi_l)} \\ \vdots \\ e^{j2\pi \frac{d}{\lambda_0}(M_2-1)\sin(\varphi_l)} \end{bmatrix}. \tag{39}$$

Further, if the range of the each target is known, say, by estimating based on the FDA-MIMO mode, then $\mathbf{a}'_{t2}$ can be obtained as

$$\mathbf{a}'_{t2}(\varphi_l) = \mathbf{r}_l^* \odot \mathbf{a}_{t2}(r_l, \varphi_l). \tag{40}$$

Accordingly, it can be derived that the steering vector of the transmit array, which relies on the angle only, can be obtained by compensating the range in $\mathbf{a}_t(r_l, \varphi_l)$ as

$$\begin{aligned} \mathbf{a}'_t(\varphi_l) &= \mathbf{c}_l \odot \mathbf{a}_t(r_l, \varphi_l) = \begin{bmatrix} \mathbf{a}_{t1}(\varphi_l) \\ \mathbf{a}'_{t2}(r_l, \varphi_l) \end{bmatrix} \\ &= \begin{bmatrix} 1 \\ e^{j2\pi \frac{d}{\lambda_0} \sin(\varphi_l)} \\ \vdots \\ e^{j2\pi \frac{d}{\lambda_0}(M-1)\sin(\varphi_l)} \end{bmatrix} \end{aligned} \tag{41}$$

where $\mathbf{c}_l = [\mathbf{1}_{M_1}^T, \mathbf{r}_l^{*T}]^T$ is a vector for range compensation. With (41), we have

$$(\mathbf{c}_l \otimes \mathbf{1}_N) \odot (\mathbf{a}_t(r_l, \varphi_l) \otimes \mathbf{a}_r(\theta_l)) = \mathbf{a}'_t(\varphi_l) \otimes \mathbf{a}_r(\theta_l)). \tag{42}$$

Now, let us define a compensation matrix $\mathbf{C} \in \mathbb{C}^{MN \times L}$ as

$$\mathbf{C} = [\mathbf{c}_1 \otimes \mathbf{1}_N, \mathbf{c}_2 \otimes \mathbf{1}_N, \ldots, \mathbf{c}_L \otimes \mathbf{1}_N]. \tag{43}$$

Then, recalling (13), we can obtain the array steering matrix $\mathbf{A}'$ of the dual-mode radar after compensation as

$$\begin{aligned} \mathbf{A}' &= \mathbf{C} \odot \mathbf{A} \\ &= [\mathbf{a}'_t(\varphi_1) \otimes \mathbf{a}_r(\theta_1)), \ldots, \mathbf{a}'_t(\varphi_L) \otimes \mathbf{a}_r(\theta_L))]. \end{aligned} \tag{44}$$

In fact, for the given eigenmatrix $\mathbf{G}_r$, the matrix $\mathbf{A}'$ can be estimated as

$$\tilde{\mathbf{A}}' = \mathbf{C} \odot (\mathbf{U}_s \mathbf{G}_r). \tag{45}$$

Similarly, let us define $\mathbf{H}_1 = [(\mathbf{I}_{M-1}, \mathbf{0}_{(M-1)\times 1}) \otimes \mathbf{I}_N]$ and $\mathbf{H}_2 = [(\mathbf{0}_{(M-1)\times 1}, \mathbf{I}_{M-1}) \otimes \mathbf{I}_N]$, we get

$$\mathbf{H}_2 \tilde{\mathbf{A}}' = \mathbf{H}_1 \tilde{\mathbf{A}}' \tilde{\mathbf{\Phi}}_{3,t} \tag{46}$$

where $\tilde{\mathbf{\Phi}}_{3,t}$ is equivalent to $\mathbf{\Phi}_{1,t}$ except for the different order of elements.

Accordingly, we obtain two matrices $\tilde{\mathbf{A}}'_{t1} \in \mathbb{C}^{(M-1)N \times 1}$ and $\tilde{\mathbf{A}}'_{t2} \in \mathbb{C}^{(M-1)N \times 1}$ as follows:

$$\tilde{\mathbf{A}}'_{t1} = \mathbf{H}_1 \tilde{\mathbf{A}}' \tag{47a}$$

$$\tilde{\mathbf{A}}'_{t2} = \mathbf{H}_2 \tilde{\mathbf{A}}' = \mathbf{H}_1 \tilde{\mathbf{A}}' \tilde{\mathbf{\Phi}}_{3,t}. \tag{47b}$$

Therefore, we have

$$\tilde{\mathbf{\Phi}}_{3,t} = (\tilde{\mathbf{A}}'^H_{t1} \tilde{\mathbf{A}}'_{t1})^{-1} \tilde{\mathbf{A}}'^H_{t1} \tilde{\mathbf{A}}'_{t2}. \tag{48}$$

Let $\tilde{\mathbf{\Phi}}_{3,t} = \mathrm{diag}\{\tilde{\rho}_{t1}, \tilde{\rho}_{t2}, \ldots, \tilde{\rho}_{tL}\}$, then the enhanced DOD obtained via MIMO and FDA-MIMO dual-mode radar can be calculated as

$$\hat{\varphi}'_l = \arcsin\left(\frac{\lambda_0 \arg(\tilde{\rho}_{tl})}{2\pi d}\right). \tag{49}$$

From (48), it can be known that matrices $\tilde{\mathbf{\Phi}}_{3,t}$ and $\mathbf{\Phi}_{1,t}$ are equivalent ones except for the different order of the diagonal elements, and both exhibit the form of a diagonal structure, then the enhanced DOD estimation of the target can be accomplished by directly selecting the diagonal elements of matrix $\tilde{\mathbf{\Phi}}_{3,t}$ without performing eigendecomposition on it. It is also noted that benefiting from the application of the eigenmatrix $\mathbf{G}_r$, the diagonal elements of the same index positions of the matrices $\tilde{\mathbf{\Phi}}_{1,t}$, $\tilde{\mathbf{\Phi}}_{2,t}$, $\tilde{\mathbf{\Phi}}_{3,t}$, and $\tilde{\mathbf{\Phi}}_r$ are bound to be guaranteed to correspond to the same target signal.

Therefore, the final DOA, DOD, and range estimation of the target signal can be given as follows:

$$\begin{cases} \hat{\theta}_l = \arcsin\left(\frac{\lambda_0 \arg(\tilde{\upsilon}_{rl})}{2\pi d}\right) \\ \hat{\varphi}'_l = \arcsin\left(\frac{\lambda_0 \arg(\tilde{\rho}_{tl})}{2\pi d}\right) \\ \hat{r}_l = \frac{c}{2\pi \Delta f} \arg(\tilde{\gamma}_l). \end{cases} \tag{50}$$

So far, it can be seen that the DOA, DOD, and range estimation of the target signal are directly completed by using the shift invariance between subarrays, which avoids the large computational burden caused by spectral peak search. At the same time, the proposed method exploits the eigenmatrix $\mathbf{G}_r$ obtained from the jointly received signal data of MIMO and FDA-MIMO dual-mode radar to achieve accurate registration of $\tilde{\mathbf{\Phi}}_r$, $\tilde{\mathbf{\Phi}}_{1,t}$, $\tilde{\mathbf{\Phi}}_{2,t}$, and $\tilde{\mathbf{\Phi}}_{3,t}$. Moreover, for the coupling of range and angle in FDA-MIMO radar mode, the proposed method converts the two-coupling problem into a single range calculation one by means of the DOD estimated in MIMO radar mode, and effectively achieves the range estimation. This process is straightforward and natural, and is able to circumvent the complex array design and corresponding multiparameter pairing problem in the bistatic FDA-MIMO radar.

Finally, the detailed steps of the proposed method for range, DOD, and DOA estimation under bistatic MIMO and FDA-MIMO dual-mode radar are shown in following the algorithm table.

C. Computational Complexity Analysis

In the proposed method, the complexity mainly stems from the construction and eigen-decomposition of the covariance matrix $\hat{\mathbf{R}}_x$, the calculation and

Algorithm 1: Joint Target Localization Method Based on Dual-Mode Radar.

Step 1: Calculate the covariance matrix $\hat{\mathbf{R}}_x = \frac{1}{J}\sum_{t_j=1}^{J}\mathbf{x}(t_j)\mathbf{x}^H(t_j)$.
Step 2: Obtain the signal subspace $\mathbf{U}_s$ from the eigen-decomposition of $\mathbf{R}_x$.
Step 3: Extract the signal subspaces $\mathbf{U}_{sr1}$ and $\mathbf{U}_{sr2}$ using (17).
Step 4: Calculate $\mathbf{\Psi}_r = (\mathbf{U}_{sr1}^H\mathbf{U}_{sr1})^{-1}\mathbf{U}_{sr1}^H\mathbf{U}_{sr2}$, and obtain the eigenmatrix $\mathbf{G}_r$ and diagonal matrix $\tilde{\mathbf{\Phi}}_r$ from the eigen-decomposition of $\mathbf{\Psi}_r$.
Step 5: Estimate the DOA $\hat{\theta}_l$ of the target signal using (22).
Step 6: Obtain the subspaces $\mathbf{U}_{1,st1}$ and $\mathbf{U}_{1,st2}$ using (26).
Step 7: Construct $\mathbf{\Psi}_{1,t} = ((\mathbf{U}_{1,st1})^H\mathbf{U}_{1,st1})^{-1}(\mathbf{U}_{1,st1})^H\mathbf{U}_{1,st2}$, and calculate $\tilde{\mathbf{\Phi}}_{1,t} = \mathbf{G}_r^{-1}\mathbf{\Psi}_{1,t}\mathbf{G}_r$ using (28).
Step 8: Calculate the subspaces $\mathbf{U}_{2,st1}$ and $\mathbf{U}_{2,st2}$ using (30).
Step 9: Construct $\mathbf{\Psi}_{2,t} = ((\mathbf{U}_{2,st1})^H\mathbf{U}_{2,st1})^{-1}(\mathbf{U}_{2,st1})^H\mathbf{U}_{2,st2}$, and calculate $\tilde{\mathbf{\Phi}}_{2,t} = \mathbf{G}_r^{-1}\mathbf{\Psi}_{2,t}\mathbf{G}_r$ using (33).
Step 10: Obtain $\tilde{\mathbf{\Gamma}} = \tilde{\mathbf{\Phi}}_{1,t}\tilde{\mathbf{\Phi}}_{2,t}^{-1}$ using (35).
Step 11: Estimate the range $\hat{r}_l$ of the target signal using (36).
Step 12: Construct the compensation matrix $\mathbf{C}$ using (43) and obtain the compensated matrix $\tilde{\mathbf{A}}'$ using (45).
Step 13: Extract matrices $\tilde{\mathbf{A}}'_{t1}$ and $\tilde{\mathbf{A}}'_{t2}$ using (47).
Step 14: Calculate $\tilde{\mathbf{\Phi}}_{3,t} = (\tilde{\mathbf{A}}'^H_{t1}\tilde{\mathbf{A}}'_{t1})^{-1}\tilde{\mathbf{A}}'^H_{t1}\tilde{\mathbf{A}}'_{t2}$.
Step 15: Estimate the enhanced DOD $\hat{\varphi}'_l$ using (49).
Step 16: Achieve the range, DOD, and DOA estimation of the target signal using (50).

eigen-decomposition of $\mathbf{\Psi}_r$, the calculation of $\mathbf{\Psi}_{1,t}$ and $\tilde{\mathbf{\Phi}}_{1,t}$, the establishment of $\mathbf{\Psi}_{2,t}$ and $\tilde{\mathbf{\Phi}}_{2,t}$, and the calculation of $\tilde{\mathbf{\Phi}}_{3,t}$. Specifically, the complexity of the construction and eigen-decomposition of the covariance matrix $\hat{\mathbf{R}}_x$ is approximately $\mathcal{O}(JM^2N^2 + M^3N^3)$. The complexity required for the computation and eigen-decomposition of $\mathbf{\Psi}_r$ is approximately $\mathcal{O}(3M(N-1)L^2 + L^3)$. The complexity of the establishment of $\mathbf{\Psi}_{1,t}$, $\tilde{\mathbf{\Phi}}_{1,t}$ and $\mathbf{\Psi}_{2,t}$, $\tilde{\mathbf{\Phi}}_{2,t}$ is approximately $\mathcal{O}(3(M_1-1)NL^2 + L^3)$ and $\mathcal{O}(3(M_2-1)NL^2 + L^3)$, respectively. The resulting complexity of the computation of $\tilde{\mathbf{\Phi}}_{3,t}$ is approximately $\mathcal{O}(3(M-1)NL^2 + L^3)$. Therefore, the computational complexity of the proposed method is approximately $\mathcal{O}(JM^2N^2 + M^3N^3 + 3(M(N-1) + (2M-3)N)L^2 + 4L^3)$. Generally, the number of elements is much larger than that of targets, i.e., $M \gg L$ and $N \gg L$. Therefore, the complexity of the proposed method can be further approximated as $\mathcal{O}(JM^2N^2 + M^3N^3)$. It can be found that the proposed method has almost similar complexity performance with the method in [37], and is significantly lower than that of the method in [38].

Furthermore, it should be emphasized that compared to the complex array structures in [37] and [38], by utilizing the designed MIMO and FDA-MIMO dual-mode radar system, the proposed method can succinctly achieve the decoupling of range and DOD in the transmit steering vector with FDA-MIMO radar mode. This does not require complex array structure design and additional parameter pairing, and can effectively complete the joint estimation of the range, DOD, and DOA of the target signal. This is extremely attractive for array design and application implementation in practical engineering.

IV. SIMULATION RESULTS

In this section, extensive simulation results are conducted to evaluate the effectiveness of the proposed target localization approach based on MIMO and FDA-MIMO dual-mode radar, including the methods in [37] and [38]. In the following simulations, the uniform linear array is employed, where the number of transmitting elements is set to 8 for both the MIMO radar and the FDA-MIMO radar. Therefore, the total number of transmitting elements with dual-mode radar is 16. The number of antennas at the receiver is also assumed to be 8. From [37] and [38], the transmit and receive antennas are set to 16 and 8, respectively, and the number of transmit subarrays employed by both is assumed to be 4. The spacing in both the transmit and receive elements of the dual-mode radar is preset to $d_t = d_r = \lambda_{\min}/2$. In addition, we assume that the carrier frequency is $f_0 = 10$ GHz and the frequency offset is $\Delta f = 15$ KHz. Unless stated otherwise, the number of snapshots is $J = 300$.

To evaluate the parameter (DOD, DOA, and range) estimation performance under the designed dual-mode radar, we adopt the root mean square errors (RMSEs), which are defined as

$$\mathrm{RMSE}_{\varphi} = \sqrt{\frac{1}{KL}\sum_{k=1}^{K}\sum_{l=1}^{L}\left(\hat{\varphi}_{l,k} - \varphi_l\right)^2} \tag{51}$$

$$\mathrm{RMSE}_{\theta} = \sqrt{\frac{1}{KL}\sum_{k=1}^{K}\sum_{l=1}^{L}\left(\hat{\theta}_{l,k} - \theta_l\right)^2} \tag{52}$$

$$\mathrm{RMSE}_{r} = \sqrt{\frac{1}{KL}\sum_{k=1}^{K}\sum_{l=1}^{L}\left(\hat{r}_{l,k} - r_l\right)^2} \tag{53}$$

where $\hat{\varphi}_{l,k}$, $\hat{\theta}_{l,k}$, and $\hat{r}_{l,k}$ stand for the estimated DOD, DOA, and range of the lth target in the kth trial, respectively. K denotes the number of Monte Carlo runs.

In the first experiment, we consider four targets located at $(-20^\circ, -38^\circ, 5000\text{ m})$, $(-16^\circ, -10^\circ, 5800\text{ m})$, $(10^\circ, 16^\circ, 7000\text{ m})$, and $(30^\circ, 45^\circ, 9000\text{ m})$. The signal-to-noise ratio (SNR) is preset to 0 dB. The resultant parameter (DOD, DOA, and range) estimation errors of the proposed approach in 50 experiments are depicted in Fig. 2, where the estimation error is defined as the difference between the parameter estimate and the true value. It can be observed from Fig. 2(a) and (b) that the fluctuation degree

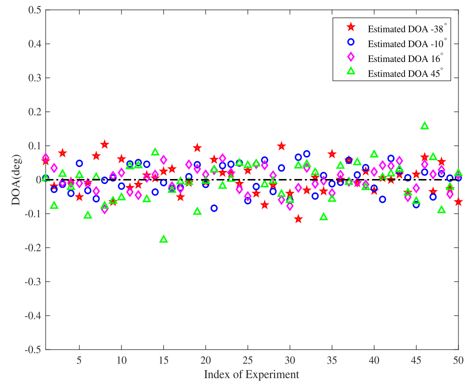

(a)

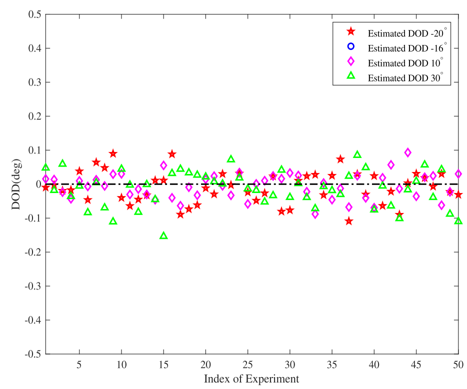

(b)

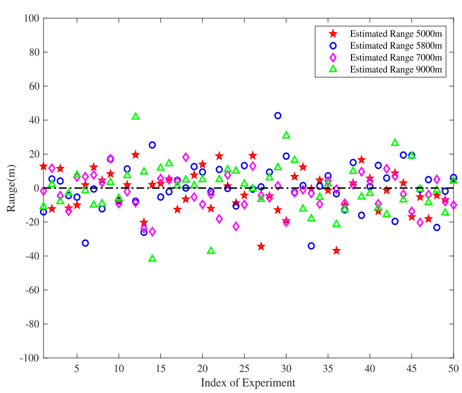

(c)

Fig. 2. Parameter (DOD, DOA, and range) estimation errors of 50 independent runs using our proposed method, where $M_1 = M_2 = 8$, $N = 8$, SNR $= 0$ dB, and $J = 300$. (a) DOA estimation. (b) DOD estimation. (c) Range estimation.

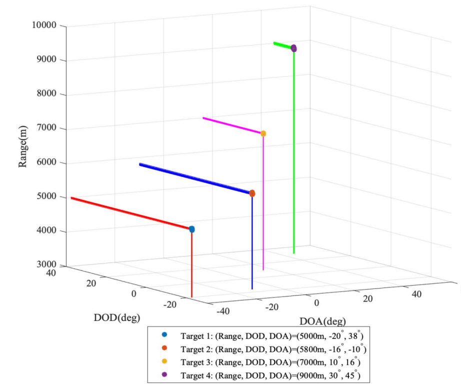

(a)

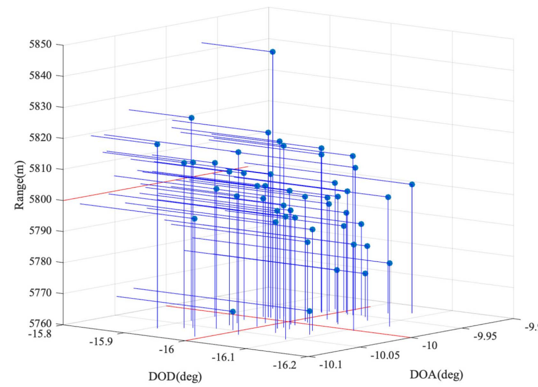

(b)

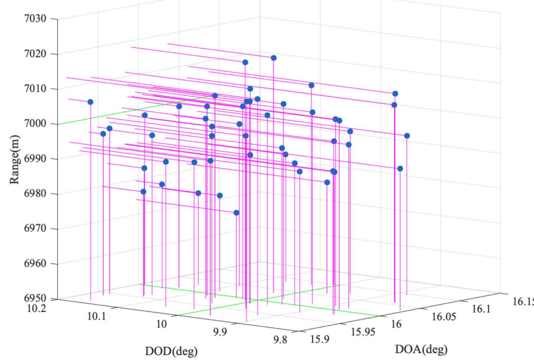

(c)

Fig. 3. Paired results of the proposed method, where $M_1 = M_2 = 8$, $N = 8$, SNR $= 0$ dB, and $J = 300$. (a) Paired results of the four targets. (b) Enlarged view of the paired result for the second target, (DOD, DOA, and range) $= (-16^\circ, -10^\circ, 5800$ m). (c) Enlarged view of the paired result for the third target, (DOD, DOA, and range) $= (10^\circ, 16^\circ, 7000\ m)$.

associated with the estimation errors of both DOA and DOD is relatively small, which exhibits a stable estimation performance. Furthermore, it can be seen from Fig. 2(c) that although the range estimation error of the target is slightly large, the result is still relatively satisfactory.

In the second experiment, we evaluate the pairing effectiveness of the proposed method in a multitarget scenario. The simulation condition is consistent with the first experiment, and Fig. 3 presents the paired results of the proposed method. It can be noticed from Fig. 3(a) that the four targets can be perfectly aligned with their respective positions by the proposed method, and there is no pairing failure. This implies that the proposed method has robust parameter pairing performance in multitarget scenarios. In addition, to show the multiparameter pairing details of the targets more clearly, we also give the enlarged view of the paired result corresponding to the second and third targets in Fig. 3(b) and (c), respectively. It can be seen that although the proposed method has a slight deviation in the parameter estimation accuracy, the targets are still able to complete the

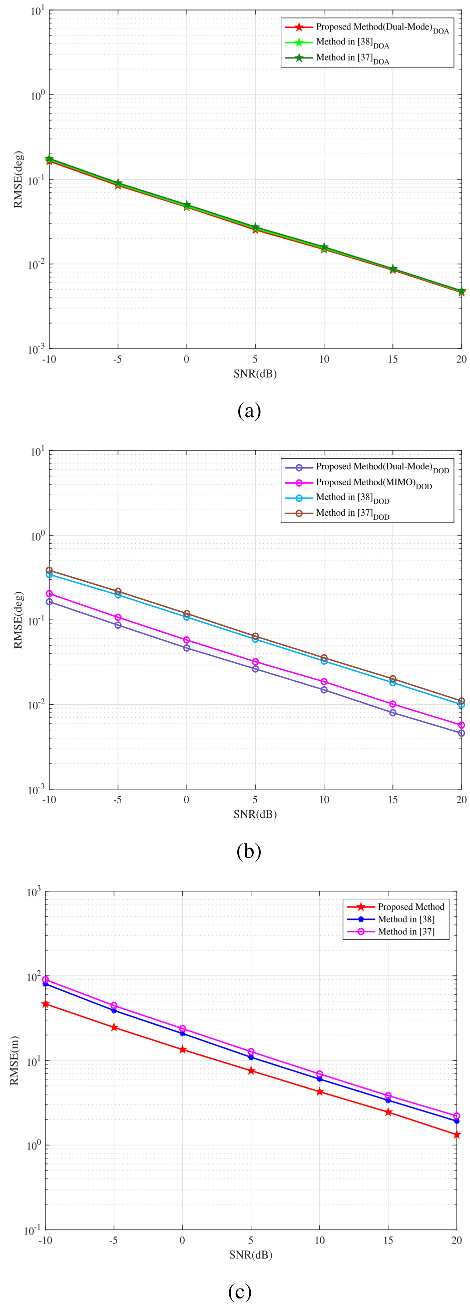

Fig. 4. RMSEs versus SNR for parameter estimation with MIMO and FDA-MIMO dual-mode radar, where $M_1 = M_2 = 8$, $N = 8$, and $J = 300$. (a) DOA estimation. (b) DOD estimation. (c) Range estimation.

correct pairing of their respective range, DOD, and DOA parameters, exhibiting extremely high accuracy.

In the third experiment, we examine the behavior of the proposed method in terms of parameter (DOD, DOA, and range) estimation RMSE. To this end, let us vary the SNR from -10 to 20 dB, and perform 500 Monte Carlo experiments. The resulting RMSEs of parameter estimation versus SNR are plotted in Fig. 4. It can be observed from Fig. 4(a) that the proposed method, the approaches in [37] and [38], are almost similar in the DOA estimation performance of the target signal. This is mainly due to the fact that they perform DOA estimation with the whole receive steering vector. Therefore, these methods are generally the same in terms of available degrees of freedom.

Interestingly, for the DOD estimation performance of target signals, the proposed approaches including dual-mode radar and MIMO radar significantly outperform the methods in [37] and [38]. This is because the two algorithms in [37] and [38] adopt the strategy of multiple subarrays on the decoupling range and DOD. Therefore, under the same number of transmit antenna configurations, the two methods are less than the proposed method in terms of the number of available array elements. Further, in extreme cases, even though they can use two subarrays to achieve the decoupling of range and DOD, their performance is inferior to the proposed method. Essentially, this comes down to the absence of this range-angle dependence in MIMO radar mode. Therefore, the proposed method can not only enjoy the advantage of MIMO radar in angle estimation but also can use this superiority for the decoupling of range and angle in FDA-MIMO radar mode. This provides a potential explanation for the excellent performance of the proposed method under MIMO and FDA-MIMO dual-mode radar system.

As expected, the performance of the DOD estimation based on the proposed dual-mode radar algorithm is significantly better than that of the proposed MIMO radar one, and is very close to the DOA estimation performance using the entire receive steering vector. This is also due to the fact that the entire transmit steering vector of the dual-mode radar can be effectively integrated by leveraging the designed range compensation factor to provide a larger array aperture utilization.

Moreover, it can be seen from Fig. 4(c) that the proposed method also significantly outperforms the methods in [37] and [38] in terms of range estimation performance. This shows that the proposed method can both retain the advantages of angle estimation provided via MIMO and FDA-MIMO dual-mode radar, while enjoying the range-dependent given via FDA radar.

In the fourth experiment, we test the performance of the proposed approach with different numbers of snapshots. In this example, the SNR is fixed at 0 dB, and the number of snapshots varies from 50 to 500. The resultant RMSEs of parameter estimation versus the number of snapshots is shown in Fig. 5. It is seen from Fig. 5(a) that the DOA estimation performance of the proposed approach, the methods in [37] and [38] has only a slight difference as the number of snapshots increases. However, for DOD estimation results, the proposed approach based on dual-mode radar and MIMO radar still outperforms the methods in [37] and [38], which is similar to the situation under SNR variation. It is also noted that the proposed algorithm based on dual-mode radar is undoubtedly the best in DOD estimation performance. This reason was also explained in the previous experiment as well.

Moreover, it can be observed from Fig. 5(c) that the range estimation performance of the proposed approach also outperforms the algorithms in [37] and [38] as the number of snapshots increases.

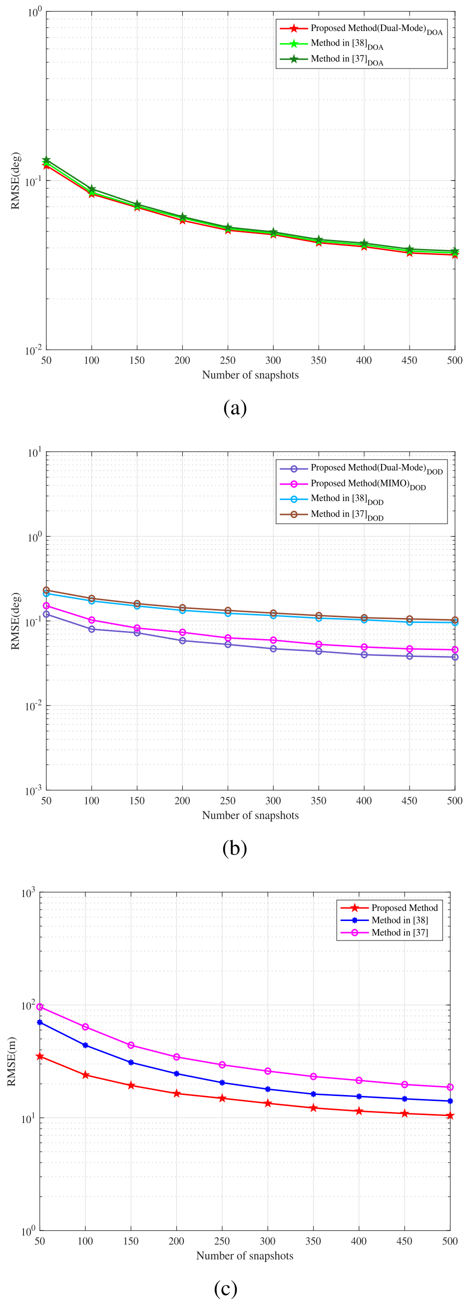

Fig. 5. RMSEs versus the number of snapshots for parameter estimation with MIMO and FDA-MIMO dual-mode radar, where $M_1 = M_2 = 8$, $N = 8$, and SNR $= 0$ dB. (a) DOA estimation. (b) DOD estimation. (c) Range estimation.

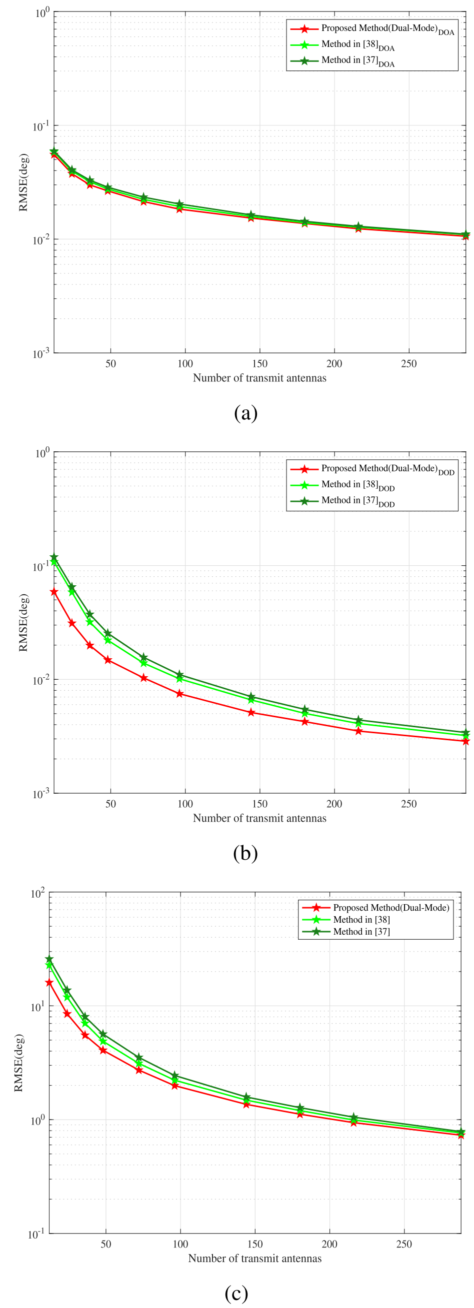

Fig. 6. RMSEs of parameter estimation versus the number of transmit antennas, where $N = 8$, SNR $= 0$ dB, and $J = 300$. (a) DOA estimation. (b) DOD estimation. (c) Range estimation.

In the fifth experiment, we evaluate the RMSE results of the proposed approach with different number of transmit antennas. Here, the transmit subarrays adopted via the methods in [37] and [38] are set to 3, but the number of elements in each subarray grows with the number of antennas in the radar configuration. Other simulation parameters are consistent with those used in Fig. 2. Fig. 6 plots the RMSE curves of these three approaches as the number of transmit antennas increases. Obviously, it can be observed from Fig. 6 that the performance improvement effect of the proposed method in both DOD and range is significant in the scenario where relatively few transmit antennas are used. In addition, it can be noticed that the performance of all methods basically tends to the same level as the number of antennas in the radar configuration increases. This can be explained that although the approaches in [37] and [38] use multiple transmit subarrays, with the increase of the number of antennas in the radar configuration, the number of available antennas in the subarrays is sufficient, which in turn can guarantee their parameter estimation performance. However, it should also be noted that the increase in the number of antennas is also a problem worthy of attention

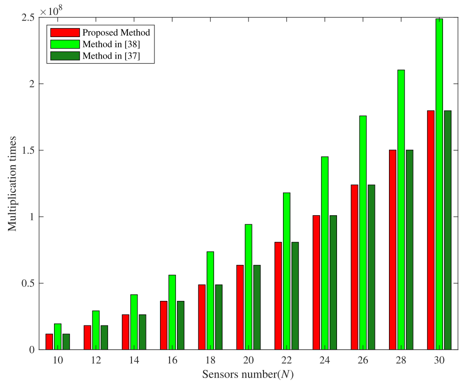

Fig. 7. Multiplication times versus N, where $M_1 = M_2 = 8$, SNR=0 dB, $J = 300$.

due to the high system cost and resource consumption requirements.

Finally, we give the approximate times of multiplication required by the corresponding method to perform parameter estimation of the target signal. In this example, the number of transmit elements is 16, of which the number of transmit antennas for both MIMO and FDA-MIMO radar is 8. For the methods in [37] and [38], the transmit array is divided into four subarrays, i.e., the number of elements in each subarray is 4. The number of receive elements is varied from 10 to 30 and the resulting multiplication times versus N are illustrated in Fig. 7. It is clearly observed that the proposed method exhibits lower complexity behavior than the method in [38], and has similar results to the method in [37]. However, it should be emphasized that compared to the methods in [37] and [38], the proposed approach is extremely attractive in terms of the improvement in both DOD and range estimation performance of the target signal.

It should also be noted that the parameter estimation performance of the three methods will tend to be the same as the number of transmit antennas increases. This can be explained that although the methods in [37] and [38] adopt multiple transmit subarrays, the performance level of these methods will basically reach a saturated state due to the sufficient number of available transmit antennas in each subarray. However, it cannot be overlooked that the large number of antennas leads to high system cost and resource consumption, which is also a point worthy of careful consideration.

V. CONCLUSION

In this article, we investigated the range-angle decoupling and target localization problems for the MIMO and FDA-MIMO dual-mode radar system. In the proposed method, bistatic MIMO and FDA-MIMO dual-mode radar model are first established. With the joint received signal data obtained via the dual-mode radar, the shift invariance between arrays is applied to estimate the DOA and the corresponding eigenmatrix of the target signal. In order to solve the coupling of range and angle in the transmit steering vector with FDA-MIMO radar mode, this eigenmatrix is constrained to the subspace data corresponding to MIMO radar and FDA-MIMO radar, respectively, to register the phase information of target signals in different radar modes. This allows us to use the DOD information provided in the MIMO radar mode to achieve the decoupling of range and angle in FDA-MIMO radar mode. This process is automatic and does not require complex array design. Moreover, we also derive a transmit steering vector synthesis algorithm based on MIMO radar and FDA-MIMO radar using the designed range compensation factor, which achieves a significant improvement in DOD estimation performance. The proposed method has a simple array geometry and does not require the cooperative work of multiple subarrays and additional parameter pairing process. The simulation results show that the proposed method significantly improves the performance of joint parameter estimation of multitarget signals and has a considerably lower computational complexity than existing methods.

It is worth noting that due to the use of the frequency increment Δf, the received signal bandwidth associated with the FDA-MIMO radar also increases as Δf becomes larger. This results in a higher Nyquist frequency. Furthermore, although the proposed approach can fully utilize the entire transmit steering vector of the FDA-MIMO radar to ensure the range estimation performance, the degree of improvement compared to DOD estimation is still limited. These disadvantages or defects will be further explored in the future.

REFERENCES

[1] H. Godrich, A. M. Haimovich, and R. S. Blum, “Target localization accuracy gain in MIMO radar-based systems,” *IEEE Trans. Inf. Theory*, vol. 56, no. 6, pp. 2783–2803, Jun. 2010.

[2] R. H. Gui, W.-Q. Wang, Y. Pan, and J. Xu, “Cognitive target tracking via angle-range-Doppler estimation with transmit subaperturing FDA radar,” *IEEE J. Sel. Topics Signal Process.*, vol. 12, no. 1, pp. 76–89, Feb. 2018.

[3] C. Cui, J. Xiong, W.-Q. Wang, and W. Wu, “Localization performance analysis of FDA radar receiver with two-stage estimator,” *IEEE Trans. Aerosp. Electron. Syst.*, vol. 54, no. 6, pp. 2873–2887, Dec. 2018.

[4] Y. F. Fang, S. Q. Zhu, C. Zeng, Y. C. Gao, and S. D. Li, “DOA estimations with limited snapshots based on improved rank-one correlation model in unknown nonuniform noise,” *IEEE Trans. Veh. Technol.*, vol. 70, no. 10, pp. 10308–10319, Oct. 2021.

[5] J. Li and P. Stoica, *MIMO Radar Signal Processing*. Hoboken, NJ, USA: Wiley, 2008.

[6] J. Li and P. Stoica, “MIMO radar with colocated antennas,” *IEEE Signal Process. Mag.*, vol. 24, no. 5, pp. 106–114, Sep. 2007.

[7] E. Fisher, A. Haimovich, R. S. Blum, L. J. Cimini, D. Chizhik, and R. A. Valenzuela, “Spatial diversity in radars models and detection performance,” *IEEE Trans. Signal Process.*, vol. 54, no. 3, pp. 823–838, Mar. 2006.

[8] W.-Q. Wang, “Phased-MIMO radar with frequency diversity for range-dependent beamforming,” *IEEE Sensors J.*, vol. 13, no. 4, pp. 1320–1328, Apr. 2013.

[9] J. J. Zhu, S. Q. Zhu, J. W. Xu, L. Lan, and X.P. He, “Cooperative range and angle estimation with PA and FDA radars,” *IEEE Trans. Aerosp. Electron. Syst.*, vol. 58, no. 2, pp. 907–921, Apr. 2022.

[10] J. Xiong, W.-Q. Wang, and K. D. Gao, “FDA-MIMO radar range-angle estimation: CRLB, MSE, and resolution analysis,” *IEEE Trans. Aerosp. Electron. Syst.*, vol. 54, no. 1, pp. 284–294, Feb. 2018.

[11] C. Wen, Y. Huang, J. Y. Peng, J. X. Wu, G. M. Zheng, and Y. H. Zhang, "Slow-time FDA-MIMO technique with application to STAP radar," *IEEE Trans. Aerosp. Electron. Syst.*, vol. 58, no. 1, pp. 74–95, Feb. 2022.

[12] R. H. Gui, W.-Q. Wang, C. Cui, and H. -C, "So, coherent pulsed-FDA radar receiver design with time-variance consideration: SINR and CRB analysis," *IEEE Trans. Signal Process.*, vol. 66, no. 1, pp. 200–214, Jan. 2018.

[13] P. Antonik, M. C. Wicks, H. D. Griffiths, and C. J. Baker, "Range dependent beamforming using element level waveform diversity," in *Proc. Int. Waveform Diversity Des. Conf.*, 2006, pp. 140–144.

[14] P. Antonik, M. C. Wicks, H. D. Griffiths, and C. J. Baker, "Frequency diverse array radars," in *Proc. IEEE Radar Conf.*, 2006, pp. 215–217.

[15] P. Antonik, M. C. Wicks, H. D. Griffiths, and C. J. Baker, "Multimission multi-mode waveform diversity," in *Proc. IEEE Radar Conf.*, 2006, pp. 580–582.

[16] S. Mustafa, D. Simsek, and H. A. E. Taylan, "Frequency diverse array antenna with periodic time modulated pattern in range and angle," in *Proc. IEEE Radar Conf.*, 2007, pp. 427–430.

[17] P. F. Sammartino, C. J. Baker, and H. D. Griffiths, "Frequency diverse MIMO techniques for radar," *IEEE Trans. Aerosp. Electron. Syst.*, vol. 49, no. 1, pp. 201–222, Jan. 2013.

[18] L. Lan et al., "GLRT-based adaptive target detection in FDA-MIMO radar," *IEEE Trans. Aerosp. Electron. Syst.*, vol. 57, no. 1, pp. 597–613, Feb. 2021.

[19] J. W. Xu, G. S. Liao, L. Huang, and H.-C. So, "Robust adaptive beamforming for fast-moving target detection with FDA-STAP radar," *IEEE Trans. Signal Process.*, vol. 65, no. 4, pp. 973–984, Feb. 2017.

[20] W.-Q. Wang, "Moving-target tracking by cognitive RF stealth radar using frequency diverse array antenna," *IEEE Trans. Geosci. Remote Sens.*, vol. 54, no. 7, pp. 3764–3773, Jul. 2016.

[21] Z. H. Mao, S.H. Liu, Y.D. Zhang, L.X. Han, and Y. M. Huang, "Joint DoA-range estimation using space-frequency virtual difference coarray," *IEEE Trans. Signal Process.*, vol. 70, pp. 2576–2592, 2022.

[22] N. Rubinstein and J. Tabrikian, "Frequency diverse array signal optimization: From non-cognitive to cognitive radar," *IEEE Trans. Signal Process.*, vol. 69, no. 1, pp. 6206–6220, Oct. 2021.

[23] L. Lan, G. S. Liao, J. W. Xu, Y. H. Zhang, and B. Liao, "Transceive beamforming with accurate nulling in FDA-MIMO radar for imaging," *IEEE Trans. Geosci. Remote Sens.*, vol. 58, no. 6, pp. 4145–4159, Jun. 2020.

[24] C. H. Wang, J. W. Xu, G. S. Liao, X. F. Xu, and Y. H. Zhang, "A range ambiguity resolution approach for high-resolution and wide-swath SAR imaging using frequency diverse array," *IEEE J. Sel. Topics Signal Process.*, vol. 11, no. 2, pp. 336–346, Mar. 2017.

[25] J. Farooq, M. A. Temple, and M. A. Saville, "Application of frequency diverse arrays to synthetic aperture radar imaging," in *Proc. Int. Conf. Electromagnetics Adv. Appl.*, 2007, pp. 447–449.

[26] J. W. Xu, G. S. Liao, S. Q. Zhu, and H.C. So, "Deceptive jamming suppression with frequency diverse MIMO radar," *Signal Process.*, vol. 113, no. 1, pp. 9–17, Aug. 2015.

[27] J. W. Xu, G. S. Liao, and H.-C. So, "Space-time adaptive processing with vertical frequency diverse array for range-ambiguous clutter suppression," *IEEE Trans. Geosci. Remote. Sens.*, vol. 54, no. 9, pp. 5352–5364, Sep. 2016.

[28] J. W. Xu, S. Q. Zhu, and G. S. Liao, "Range ambiguous clutter suppression for airborne FDA-STAP radar," *IEEE J. Sel. Topics Signal Process.*, vol. 9, no. 8, pp. 1620–1631, Dec. 2015.

[29] W.-Q. Wang and H. Shao, "Range-angle localization of targets by a double pulse frequency diverse array radar," *IEEE J. Sel. Topics Signal Process.*, vol. 8, no. 1, pp. 106–114, Feb. 2014.

[30] W.-Q. Wang, "Subarray-based frequency diverse array radar for target range-angle estimation," *IEEE Trans. Aerosp. Electron. Syst.*, vol. 50, no. 4, pp. 3057–3067, Oct. 2014.

[31] W.-Q. Wang, "Range-angle dependent transmit beampattern synthesis for linear frequency diverse arrays," *IEEE Trans. Antennas Propag.*, vol. 61, no. 8, pp. 4073–4081, Aug. 2013.

[32] W.-Q. Wang and H. C. So, "Transmit subaperturing for range and angle estimation in frequency diverse array radar," *IEEE Trans. Signal Process.*, vol. 62, no. 8, pp. 2000–2011, Apr. 2014.

[33] J. Xu, G. Liao, S. Zhu, L. Huang, and H.C. So, "Joint range and angle estimation using MIMO radar with frequency diverse array," *IEEE Trans. Signal Process.*, vol. 63, no. 13, pp. 3396–3410, Jul. 2015.

[34] W. Khan, I. M. Qureshi, and S. Saeed, "Frequency diverse array radar with logarithmically increasing frequency offset," *IEEE Antennas Wireless Propag. Lett.*, vol. 14, pp. 499–502, 2015.

[35] Y. Liu, H. Ruan, L. Wang, and A. Nehorai, "The random frequency diverse array: A new antenna structure for uncoupled direction-range indication in active sensing," *IEEE J. Sel. Topics Signal Process.*, vol. 11, no. 2, pp. 295–308, Mar. 2017.

[36] S. Qin, Y. D. Zhang, M. G. Amin, and F. Gini, "Frequency diverse coprime arrays with coprime frequency offsets for multitarget localization," *IEEE J. Sel. Topics Signal Process.*, vol. 11, no. 2, pp. 321–335, Mar. 2017.

[37] C. Cui, J. Xu, R. H. Gui, W.-Q. Wang, and W. Wu, "Search-free DOD, DOA and range estimation for bistatic FDA-MIMO radar," *IEEE Access*, vol. 6, pp. 15431–15445, 2018.

[38] F. L. Liu, X. P. Wang, M. X. Huang, and L. T. Wan, "Joint angle and range estimation for bistatic FDA-MIMO radar via real-valued subspace decomposition," *Signal Process.*, vol. 185, no. 1, Aug. 2021, Art. no. 108065.

[39] C. Wang, X. F. Zhang, and J. F. Li, "FDA-MIMO radar for DOD, DOA, and range estimation: SA-MCFO framework and RDMD algorithm," *Signal Process.*, vol. 188, no. 1, Nov. 2021, Art. no. 108209.

[40] C. Wen, C. Z. Ma, J. Y. Peng, and J. X. Wu, "Bistatic FDA-MIMO radar space-time adaptive processing," *Signal Process.*, vol. 163, no. 1, pp. 201–212, Oct. 2019.

[41] R. Roy and T. Kailath, "ESPRIT-estimation of signal parameters via rotational invariance techniques," *IEEE Trans. Acoust. Speech Signal Process.*, vol. 37, no. 7, pp. 984–995, Jul. 1989.

Yunfei Fang received the M.S. degree from the College of Information Engineering from Dalian University, Dalian, China, in 2018, and the Ph.D. degree from the National Laboratory of Radar Signal Processing, Xidian University, Xi'an, China, in 2023, both in electrical engineering.

His research interests include spectral estimation, array signal processing, frequency diverse array, and multiple-input–multiple-output Radar.

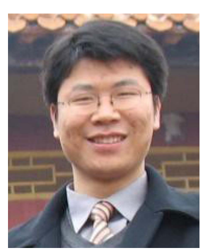

Shengqi Zhu (Senior Member IEEE) received the B.S. and Ph.D. degrees in electrical engineering from Xidian University, Xi'an, China, in 2005 and 2010, respectively.

He is currently a Professor with Xidian University. His research interests include wave diversity radars, with an emphasis on frequency diverse arrays, time diverse arrays, and element-pulse coding array radars, adaptive signal processing, synthetic aperture radar ground-moving target indication, and sparse signal processing.

Bin Liao (Senior Member IEEE) received the B.Eng. and M.Eng. degrees from Xidian University, Xi'an, China, in 2006 and 2009, respectively, and the Ph.D. degree from the University of Hong Kong, Hong Kong, in 2013, all in electrical engineering.

From 2013 to 2014, he was a Research Assistant with the Department of Electrical and Electronic Engineering, The University of Hong Kong, where he was also a Research Scientist with the Department of Electrical and Electronic Engineering, in 2016. In 2023, he was a Visiting Professor with the Centre for Wireless Innovation, Queen's University Belfast, Belfast, U.K. He is currently a Full Professor with the College of Electronics and Information Engineering, Shenzhen University, Shenzhen, China. His research interests include sensor array processing, adaptive filtering, and convex optimization, with applications to radar, navigation, and communications.

Dr. Liao was the recipient of the Best Paper Award in the 2016 21st International Conference on Digital Signal Processing and the 2017 22nd International Conference on Digital Signal Processing. He was also the recipient of the National Natural Science Foundation of China and European Research Council programme . He is an Associate Editor for IEEE TRANSACTIONS ON AEROSPACE AND ELECTRONIC SYSTEMS, *IET Signal Processing*, and *Multidimensional Systems and Signal Processing*.

Ximin Li was born in Liao Cheng, China, in 1983. He received the B.S. degree in radar engineering, the M.S. degree in microwave technology, and the Ph.D. degree in electromagnetic field from the Air Force Engineering University, Xi'an, China, in 2005, 2008, and 2011, respectively.

He is currently an Associate Professor with the National Laboratory of Radar Signal Processing, Xidian University, Xi'an. His research interests include array signal processing, target electromagnetic scattering modeling, waveform diversity radar antijamming.

Guisheng Liao (Senior Member IEEE) was born in Guilin, Guangxi, China, in 1963. He received the B.S. degree in mathematics from Guangxi University, Guangxi, in 1985, and the M.S. degree in computer science and the Ph.D. degree in electrical engineering from Xidian University, Xi'an, China, in 1990 and 1992, respectively.

From 1999 to 2000, he was a Senior Visiting Scholar with the Chinese University of Hong Kong, Hong Kong. Since 2006, he has been a Panelist for the medium and long term development plan in high-resolution and remote sensing systems. Since 2007, he has been the Lead of Yangtze River Scholars Innovative Team and devoted in advanced techniques in signal and information processing. Since 2009, he has been the Evaluation Expert for the international cooperation project of the Ministry of Science and Technology in China. He is currently a Yangtze River Scholars Distinguished Professor with the National Laboratory of Radar Signal Processing and serves as the Dean of the Hangzhou Institute of Technology, Xidian University. His research interests include array signal processing, space-time adaptive processing, radar waveform design, and airborne/space surveillance, and warning radar systems.